


22 **Abstract**

23 Optimum performance of irrigated crops in regions with shallow saline groundwater
24 requires a careful balance between application of irrigation water and upward
25 movement of salinity from the groundwater. Few field validated surrogate models are
26 available to aid in the management of irrigation water under shallow groundwater
27 conditions. The objective of this research is to develop a model that can aid in the
28 management using a minimum of input data that is field validated. In this paper a
29 2-year field experiment was carried out in the Hetao irrigation district in Inner
30 Mongolia, China and a physically based integrated surrogate model for arid irrigated
31 areas with shallow groundwater was developed and validated with the collected field
32 data. The integrated model that links crop growth with available water and salinity in
33 the vadose zone is called Evaluation of the Performance of Irrigated Crops and Soils
34 (EPICS). EPICS recognizes that field capacity is reached when the matric potential is
35 equal to the height above the groundwater table and thus not by a limiting hydraulic
36 conductivity. In the field experiment, soil moisture contents and soil salt conductivity
37 at 5 depths in the top 100 cm, groundwater depth, crop height, and leaf area index
38 were measured in 2017 and 2018. The field results were used for calibration and
39 validation of EPICS. Simulated and observed data fitted generally well during both
40 calibration and validation. The EPICS model that can predict crop growth, soil water,
41 groundwater depth and soil salinity can aid in optimizing water management in
42 irrigation districts with shallow aquifers.

43 **Key words:** Surrogate hydrological model, irrigated crops, shallow aquifer

Summary of comments: hess-2019-656-manuscript-version5.pdf

Page:2

 Number: 1 Author: Subject: Highlight Date: 2020-06-18 16:41:32

In light of the many uses for the word performance, perhaps "optimum management of irrigated crops" would be more straightforward.

Nomenclature			
ET_0	Reference evapotranspiration (mm)	p	Fraction of readily available soil water relative to the total available soil water
ET_P	Potential evapotranspiration (mm)	S	Salt stress coefficient ()
E_p	Potential evaporation (mm)	B	Crop specific parameter (%)
T_p	Potential transpiration (mm)	k_y	Factor that affects crop yield
E_a	Actual evaporation (mm)	EC_{Ce}	Electrical conductivity of the soil saturation extract (mS cm ⁻¹)
T_a	Actual transpiration (mm)	$EC_{ethreshold}$	Threshold of the electrical conductivity of the soil saturation extract when the crop yield becomes affected by salt (mS cm ⁻¹)
K_c	Crop coefficient()	$EC_{1:5}$	Electrical conductivity of the soil extract that soil samples mixed with distilled water in a proportion of 1:5 (mS cm ⁻¹)
τ	Development stage of the leaf canopy()	θ_s	Soil moisture content at saturation (cm ³ cm ⁻³)
r_T	Root function for transpiration ()	ϕ_b	Bubbling pressure (cm)
r_E	Root function for evaporation ()	ϕ_m	Matric potential (cm)
j	Number of soil layer()	λ	Pore size distribution index
LAI	Leaf area index()	h	Groundwater depth (cm)
T_{mean}	Mean daily temperature (°C)	z	Depth of the point below the soil surface (cm)
T_{mx}	Maximum daily temperature (°C)	$Wfc(h)$	Total water content at field capacity of the soil profile over a prescribed depth (cm)
T_{mn}	Minimum daily temperature (°C)	$L(j)$	Height of layer j (cm)
LAI_{mx}	Maximum leaf area index	μ	Drainable porosity
RD_{mx}	Maximum root depth (cm)	P	Precipitation (mm)
K_b	Dimensionless canopy extinction coefficient	I	Irrigation (mm)
PHU	Total potential heat units required for crop maturation (°C)	n	Number of soil layers
Z_{1j}	Depth of the upper boundaries of soil layer j (cm)	R_{gw}	Percolation to groundwater (mm)
Z_{2j}	Depth of the lower boundaries of the soil layer for $r_E(j,t)$; root depth or the lower boundaries of the soil layer for $r_T(j,t)$ (cm)	$R_w(j-1,t)$	Percolation rate to layer j from layer j-1 at day t (mm)
δ	Water use distribution parameter	$C(j,t)$	Salt concentration of layer j at day t (g L ⁻¹)
k_E	Water stress coefficient for evaporation	C_i	Salt concentration of irrigation water (g L ⁻¹)
k_T	Water stress coefficient for transpiration	C_{gw}	Salt concentration of groundwater (g L ⁻¹)
θ	Soil moisture content (cm ³ cm ⁻³)	U_{gw}	Actual upward flux of groundwater (mm)
θ_{fc}	Soil moisture content at field capacity (cm ³ cm ⁻³)	$U_{gw,max}$	Maximum upward flux of groundwater (mm)
θ_r	Soil moisture content at wilting point (cm ³ cm ⁻³)	a	Constant used for calculation of $U_{gw,max}$ ()
f_{shape}	Shape factor of kT curve ()	b	Constant used for calculation of $U_{gw,max}$ ()

45 1. Introduction

46 Irrigation water is a scarce resource, especially in arid and semi-arid areas of the
47 world. Irrigation improves quality and quantity of food production; however, excess
48 irrigation and salinization remain one of the key challenges. Almost 20% of the
49 irrigated land in the world is affected by salinization and this percentage is still on the
50 rise (Li et al., 2014). Salinity affects agricultural production¹(Williams, 1999). Soil
51 salinization and water shortages, especially associated with surface irrigated
52 agriculture in arid to semi-arid areas, is a threat to the well-being of local communities
53 in these areas (Dehaan and Taylor, 2002; Rengasamy, 2006).

54 In arid and semi-arid surface irrigation³with flood irrigation²and districts without a
55 drainage infrastructure, the groundwater table is close to the surface because more
56 water has been applied than crop evapotranspiration. Capillary rise of the shallow
57 groundwater can be used to supplement irrigation and thereby, in closed basins, can
58 possibly save water for irrigating additional areas downstream (Gao et al., 2015; Yeh
59 and Famiglietti, 2009; Luo and Sophocleous, 2010.). However, at the same time,
60 capillary upward moving water carries salt from the groundwater increasing the salt in
61 the upper layers of the soil leading to soil degradation and possibly decreasing yields
62 and change of crop patterns to more salt tolerant crops (Guo et al., 2018; Huang et al.,
63 2018). The leaching of salts with irrigation water is necessary and useful for irrigated
64 agriculture (Letey et al., 2011). In north China, the fields are commonly irrigated in the
65 autumn before soil freezing to leach salts and provide water for first growth after
66 deeding⁴in the following year (Feng et al., 2005; Pereira et al., 2007).

 Number: 1 Author: Subject: Highlight Date: 2020-06-18 16:43:55

This is repetitive of the previous sentence.

 Number: 2 Author: Subject: Highlight Date: 2020-06-18 16:51:43

In my previous comments, I mentioned that it would help some readers if surface irrigation was distinguished from irrigation supplied from surface water sources (as opposed to groundwater sources). Although the authors have clarified that this research was conducted in flood irrigated fields, I think this is still pertinent in this introduction to differentiate the irrigation methods from the source water when using the term "surface irrigation". This is especially relevant here because saline groundwater complicate the management salinity, regardless of irrigation technique (flood/surface, sprinkler, sub, or drip).

 Number: 3 Author: Subject: Highlight Date: 2020-06-18 16:44:20

 Number: 4 Author: Subject: Highlight Date: 2020-06-18 16:57:58

89 These integrated models require input data that are usually not available when
90 applied over extended areas (Liu et al., 2009; Xu et al., 2016; Hu et al., 2019). The
91 EPIC crop growth model is often preferred in integrated crop growth hydrology
92 models because it requires relatively few input data and is accurate (Wang et al.,
93 2014; Xu et al., 2013; Chen et al., 2019).

94 There is a tendency with the advancement of computer technology to include
95 more physical processes in these models (Asher et al., 2015; Doherty and Simmons,
96 2013; Leube et al., 2012). Detailed spatially input of soil hydrological properties and
97 crop growth are required to take advantage of the model complexity (Flint et al., 2002;
98 Rosa et al., 2012). This greater model complexity, both in space and time, requires
99 longer model run times, especially for the time-dependent models (Leube et al., 2012).
100 These models are useful for research purposes but for actual field applications, the
101 required input data are not available and expensive to obtain. In such cases, simpler
102 surrogate models are a good alternative (Blanning, 1975; Willcox and Peraire, 2002;
103 Regis and Shoemaker, 2005). Surrogate models run faster and are as accurate as
104 the complex models for a specific problem (shallow groundwater here) but not as
105 versatile as the more complex models that can be applied over a wide range of
106 conditions (Asher et al., 2015).

107 Simple surrogate models are abundant in China for areas where the groundwater
108 is deeper than approximately 10 m (Kendy et al., 2003; Chen et al., 2010; Ma et al.,
109 2013; Li et al., 2017; Wu et al., 2016), but are limited and relatively scarce for areas
110 where the groundwater is near the surface in the arid to semi-arid areas (Xue et al.,

133 model less useful for practical application.

134 Because of the shortcomings in the above complex models, we avoided the use
135 of a constant drainable porosity and considered the crop growth and thus improved
136 the surrogate model in our last study (Liu et al., 2019). The objective of this research
137 was to develop a field validated surrogate model that could be used to simulate the
138 water and salt movement and crop growth in irrigated areas with shallow groundwater
139 and salinized soil with a minimum of input parameters. To validate the surrogate
140 model, we performed a 2-year field experiment in the Hetao irrigation district that
141 investigated the change in soil salinity, moisture content, groundwater depth and
142 maize and sunflower growth during the growing season.

143 In the following section we present first the theoretical background of the
144 surrogate model. The model consists of crop growth module and a vadose zone
145 module. This is followed by detailed description of the two-year field experiments
146 starting in 2017 in the Hetao irrigation district where maize and sunflower were
147 irrigated by flooding the field. The experimental results consisting of climate data,
148 irrigation application, crop growth parameters, moisture and salt content and
149 groundwater depth are used to calibrate and validate the model.

150 **2. Model description**

151 2.1 Introduction of the model

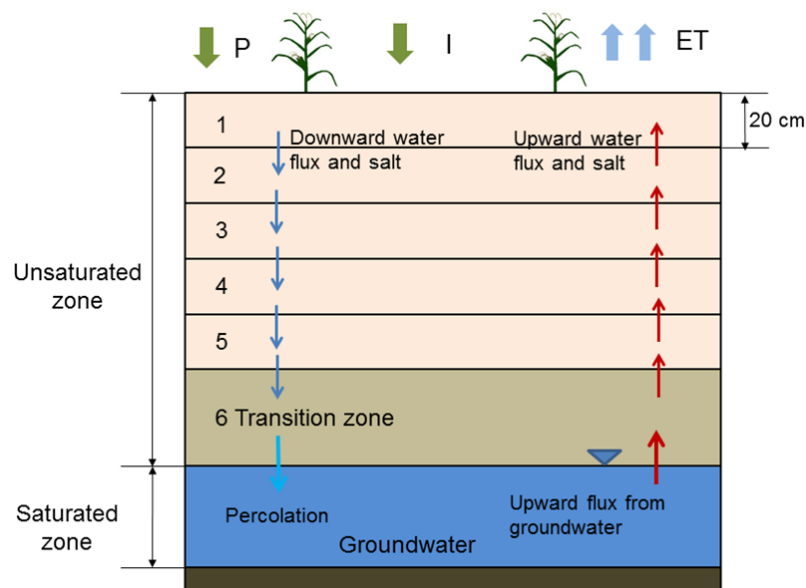
152 In a recent study, we presented a surrogate model for the vadose zone with shallow
153 groundwater using the novel concept that the moisture content at field capacity is a
154 unique function of the groundwater depth after irrigation or precipitation that wets up


155 the entire soil profile. The model, called the Shallow Vadose Groundwater model,
 156 applies directly to surface irrigated districts where the groundwater is within 3.3 m
 157 from the soil surface (Liu et al. 2019). The model was a proof of concept with
 158 calibrated values for evapotranspiration and soil salinity and was not simulated.

159 To make the Shallow Vadose Groundwater model more physically realistic, we
 160 added a crop growth model and included the effect of salinity and moisture content on
 161 evaporation and transpiration directly in this study. The new model that combines
 162 parts of the Environmental Policy Integrated Climate (EPIC) with Shallow Vadose
 163 Groundwater model is called the *Evaluation of the Performance of Irrigated Crops*
 164 *and Soils* (EPICS).

165 2.2 Structure of the EPICS model

166 In the EPICS model, the soil profile is divided into five layers of 20 cm (from the soil
 167 surface down) and a sixth layer that stretches from the 100 cm depth to the water
 168 table below (Fig. 1).



 Number: 1 Author: Subject: Highlight Date: 2020-06-18 17:51:17

 Number: 2 Author: Subject: Highlight Date: 2020-06-18 17:57:13

This acronym is applied inconsistently throughout the text. See lines 219-220. Since your model acronym (EPICS) is very similar, I suggest that you ensure that this is correct and consistent to help the reader keep it all straight.

199 upward flux is less than the actual evapotranspiration.

200 Finally, the link between the VADOSE and the CROP modules is achieved by
201 calculating the actual evapotranspiration with parameters of both modules consisting
202 of the moisture content and the salt content simulated in the VADOSE module and
203 root distribution and potential evapotranspiration in the CROP module (Fig. 2).

204 2.3 Theoretical background of the EPICS model

205 In the next section, the equations of the CROP in the VADOSE modules are
206 presented. The calculations are carried out sequentially on a daily time step. [This](#)
207 [model predicts field daily soil water, salt content and crop growth, which are critical](#)
208 [parameters for irrigation water management. For field and regional water](#)
209 [management and irrigation policy development, resolution of daily time step is](#)
210 [sufficient.](#) Finer resolution is not needed for managing water and salt content for
211 irrigation. In the first step, the actual evaporation and transpiration are calculated for
212 each layer in the model. Next, the moisture content and salt content are adjusted for
213 the various fluxes. Since the equations for the downward movement on days of
214 rainfall and/or irrigation are different than for upward movement from the groundwater
215 on the remaining days, we present upward and downward movement in separate
216 sections. The code was written in Matlab 2014Ra and Microsoft Excel was used for
217 data input and output.

218 2.3.1 CROP module

219 The crop module uses functions of EPIC ([Erosion Productivity Impact Calculator](#))¹

This acronym is defined inconsistently here and above. This is the correct attribution from Williams et al., 1989. See line 162.

$$k_T(j, t) = 1 - \frac{\exp\left[\left(1 - \frac{\theta(j, t) - \theta_r(j)}{(1-p)[\theta_{fc}(j) - \theta_r(j)]}\right) f_{shape}\right] - 1}{\exp(f_{shape}) - 1} \quad \theta \leq \theta_{fc} \quad (5a)$$

$$k_T(j, t) = 1 \quad \theta > \theta_{fc} \quad (5b)$$

257 where f_{shape} is the shape factor of $k_T(j, t)$ curve, p is the fraction of readily
 258 available soil water relative to the total available soil water. Finally, the salt stress
 259 coefficient $S(j, t)$ for each layer in Eq 3b can be calculated as (Allen et al., 1998; Xue
 260 et al., 2018):

$$S(j, t) = 1 - \frac{B}{100 k_y} (EC_e(j, t) - EC_{ethreshold}) \quad (6)$$

261 where k_y is the factor that affects the yield, EC_e is the electrical conductivity of the
 262 soil saturation extract (mS cm^{-1}), $EC_{ethreshold}$ is the calibrated threshold of the
 263 electrical conductivity of the soil saturation extract when the crop yield becomes
 264 affected by salt (mS cm^{-1}), and B is the calibrated crop specific parameter that
 265 describes the decrease rate of crop yield when EC_e increases per unit below the
 266 threshold. The electrical conductivity of the soil saturation extract can be calculated
 267 as (Rhoades et al., 1989):

$$EC_e = 1.33 + 5.88 \times EC_{1:5} \quad (7)$$


268 where $EC_{1:5}$ is the electrical conductivity of the soil extract that soil samples mixed
 269 with distilled water in a proportion of 1:5.

270 2.3.2 VADOSE Module

271 For modeling the daily soil moisture content and groundwater depth, first we need

272 calculate the soil moisture content at field capacity and the drainable porosity based

273 on the soil moisture characteristic curve. Besides, considering the water and salt

274 movement is different when there have¹ irrigation and/or precipitation, we simulate the
275 daily soil moisture content and salt with downward flux or upward flux. ²

276 2.3.2.1 Parameters based on soil moisture characteristic curve for modeling

277 Moisture content at field capacity


278 Field capacity with a shallow groundwater is different than in soils with deep
279 groundwater where water stops moving when the hydraulic conductivity becomes
280 limiting at -33 kPa. When the groundwater is shallow, the hydraulic conductivity is not
281 limiting and the water stops moving when the hydraulic potential is constant and thus
282 the matric potential is equal to the height above the water table (Gardner 1958;
283 Gardner et al., 1970a, b; Steenhuis et al. 1988; Liu et al., 2019). Assuming a unique
284 relationship between moisture content at field capacity and matric potential (i.e. soil
285 characteristic curve), the moisture content at field capacity at any point above the
286 water table is a unique function of the water table depth. Thus, any water added
287 above field capacity will drain downward. When the groundwater is recharged, the
288 water table will rise and increase the moisture contents at field capacity throughout
289 the profile.


290 The moisture contents at field capacity were found by Liu et al. (2019) using the
291 simplified Brooks and Corey soil characteristic curve (Brooks and Corey, 1964)

$$\theta = \theta_s \left[\frac{\varphi_m}{\varphi_b} \right]^{-\lambda} \quad \text{for } |\varphi_m| > |\varphi_b| \quad (8a)$$

$$\theta = \theta_s \quad \text{for } |\varphi_m| \leq |\varphi_b| \quad (8b)$$

292 in which θ is the soil moisture content ($\text{cm}^3 \text{ cm}^{-3}$), θ_s is the saturated moisture

 Number: 1 Author: Subject: Highlight Date: 2020-06-18 19:58:39

 Number: 2 Author: Subject: Note Date: 2020-06-18 20:17:09

Lines 271-275: Both of these sentences have multiple grammatical errors, and should be reviewed to ensure that the authors' intended meaning is correctly stated.

312 The drainable porosity is a crucial parameter in modelling the groundwater depth and
313 soil moisture content. According to the soil water characteristic curve at field capacity,
314 the drainable porosity can be expressed as a function of the depth. The drainable
315 porosity is obtained by calculating the field capacity, $W_{fc}(h)$ (cm) for each layer at all
316 groundwater depths. The total water content at field capacity of the soil profile over a
317 prescribed depth with a water table at depth h can be expressed as:

$$W_{fc}(h) = \sum_{j=1}^n [L(j) \theta_{fc}(j, h)] \quad (10)$$

318 where $\theta_{fc}(j, h)$ is the average moisture content at field capacity of layer j that can be
319 found by integrating Eq. 8 from the upper to the lower boundary of the layer and
320 dividing by the length $L(j)$ which is the height of layer j . The matric potential at the
321 boundary is equal to the height above the water table. The drainable porosity, $\mu(h)$,
322 which is a function of the groundwater depth h , can simply be found as the difference
323 in water content when the water table is lowered over a distance of $2\Delta h$.

$$\mu(h) = \frac{W_{fc}(h + \Delta h) - W_{fc}(h - \Delta h)}{2\Delta h} \quad (11)$$

324 where $\Delta h = 0.5L(j)$ (cm).

325 **2.3.2.2 Downward flux (at times of irrigation and/or precipitation) and model output**

326 At this situation, the model can simulate the daily soil moisture content of different
327 layer, the percolation from the upper layer to the next layer, the recharge to the
328 groundwater, the soil salt concentration of different layer and the salt concentration of
329 groundwater and the groundwater depth.

330 **Water**

This sentence has multiple grammatical errors.

367 2018), $C_{gw}(t)$ is the soluble salt concentration of groundwater at day t (g L^{-1}).

368 2.3.2.3 Upward flux and model output

369 For the upward flux period, the downward water flux to groundwater is zero. The
370 evapotranspiration leads to the decrease of soil moisture content in the vadose zone
371 and lowers the groundwater table due to the upward movement of groundwater to
372 crop root zone and soil surface. The soil moisture content is calculated by taking the
373 difference of equilibrium moisture content associated with the change of groundwater
374 depth. At this situation, the model can output the daily soil moisture content of
375 different layer, the upward groundwater flux, the groundwater depth, the soil salt
376 concentration of different layer and the salt concentration of groundwater.

377 Water

378 The groundwater upward flux, $U_{gw}(h, t)$, is limited by either the maximum upward
379 flux of groundwater, $U_{gw,max}(h)$, or the actual evapotranspiration, formally stated as:

$$U_{gw}(h, t) = \min [[E_a(t) + T_a(t)], U_{gw,max}(h)] \quad (20)$$

$$E_a(t) = \sum_{j=1}^n E_a(j, t) \quad (21)$$

$$T_a(t) = \sum_{j=1}^n T_a(j, t) \quad (22)$$

380 where $U_{gw,max}(h)$ is the actual upward flux from groundwater (mm), $E_a(t)$ is the
381 actual evaporation at day t (mm), $T_a(t)$ is the actual transpiration at day t (mm),
382 $E_a(j, t)$ is the actual evaporation at day t of layer j (mm) and $T_a(j, t)$ is the actual
383 transpiration at day t of layer j (mm).

384 The maximum upward flux can be expressed as (Liu et al., 2019; Gardner et al.,

As in the section above, please fix grammatical errors in this sentence.

402 the moisture content is updated with the difference between the two fluxes,
 403 $U_{gw,max}(h)$ and $[E_a(t) + T_a(t)]$, according to a predetermined distribution extraction of
 404 water out of the root zone

$$\theta(j, t) = \theta(j, t - \Delta t) + \theta_{fc}(j, h(t)) - \theta_{fc}(j, h(t - \Delta t)) - \frac{r(j)[E_a(t) + T_a(t) - U_{gw,max}(h)]}{L(j)} \quad (27)$$

405 The upward flux of water can be found by summing the differences in moisture
 406 content above the layer j similar to Eq 14, but starting the summation at the
 407 groundwater.

408 **Salinity**

409 The salt from groundwater is added to the soil layers according to the root function.

410 The soil salinity concentration in layer j at day t can be expressed as

$$C(j, t) = \frac{\theta(j, t - \Delta t) C(j, t - \Delta t) L(j) + r(j, t) U_g(h, t) C_{gw}(t)}{\theta(j, t - \Delta t) L(j) + (\theta_{fc}(j, h(t)) - \theta_{fc}(j, h(t - \Delta t))) L(j) - r(j, t) (E_a(t) + T_a(t) - U_{gw,max}(h))} \quad (28)$$

411 Since water is extracted from the reservoir that has the same concentration as in the
 412 reservoir, the concentration will not change, hence the equation used to estimate the
 413 groundwater salt concentration can be expressed as

$$414 \quad C_{gw}(t) = C_{gw}(t - \Delta t) \quad (29)$$

415 **3. Data collection**

416 **3.1 Study area**

417 Field experiments were conducted in 2017 and 2018 in Shahaoqu experimental
 418 station in Jiefangzha sub-district, Heato irrigation district in Inner Mongolia, China (Fig.
 419 3). Irrigation water originates from the Yellow River. The area has an arid continental
 420 climate. Mean annual precipitation is 155 mm a⁻¹ of which 70% falls from June to
 421 September. Pan evaporation is 2000 mm a⁻¹ (Xu et al., 2010). The mean annual

Does salinity of this source water change seasonally?

437 planted with gourds and were therefore not monitored in 2018. Fields B and C were
 438 seeded with sunflower in both 2017 and 2018. The sunflower was planted on June 1,
 439 2017 and June 5, 2018. Harvest was on September 15 in both years. The fields were
 440 irrigated by flooding the field ranging from two to five times during the growing season
 441 (Table 1). A well was installed in each experimental field to monitor the groundwater
 442 depth.

443 Table 1 Irrigation scheduling for the Shahaoqu experimental fields in 2017 and 2018

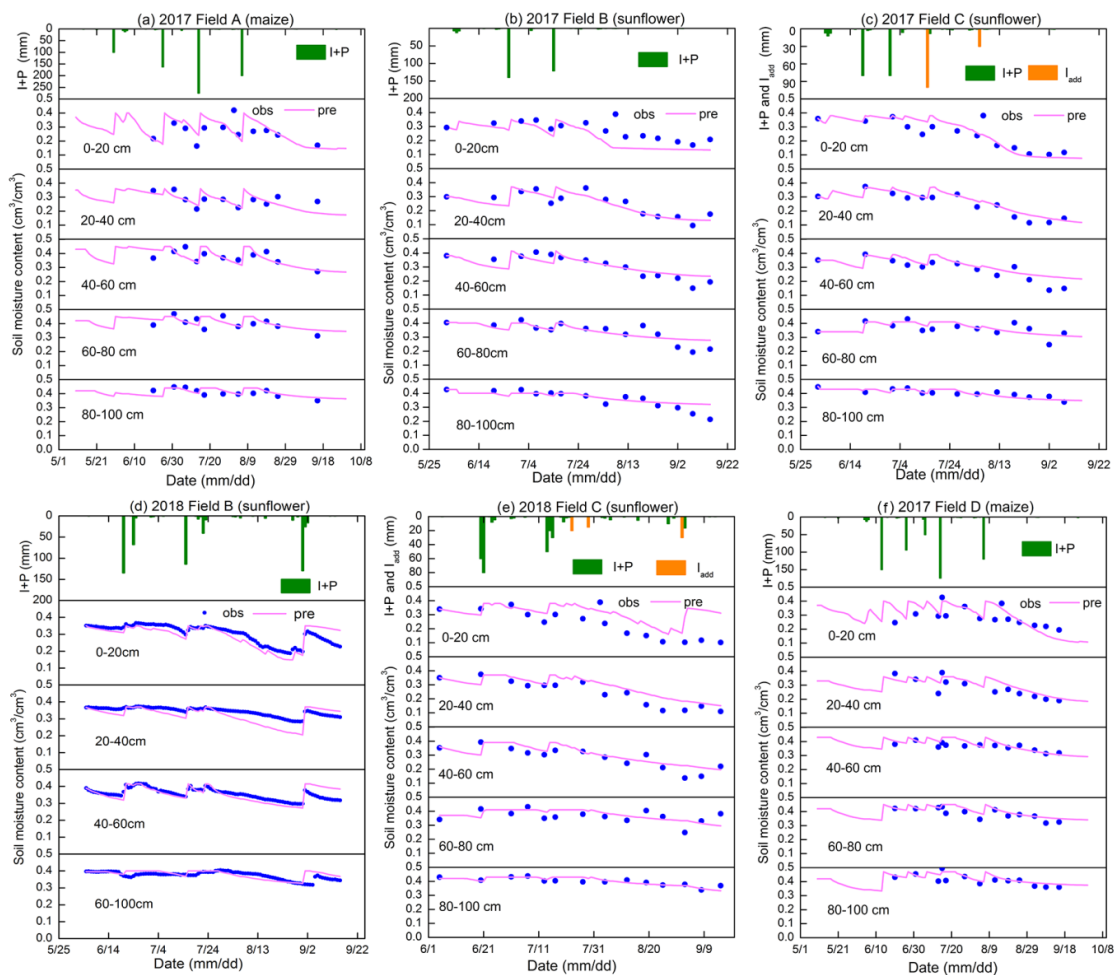
Field	Year	Irrigation events	Date	Irrigation depth (mm)
A (maize)	2017	1	5/30	100
		2	6/25	162
		3	7/14	275
		4	8/6	199
	2017	1	6/26	140
		2	7/23	121
B (sunflower)	2018	1	6/20	134
		2	6/24	60
		3	7/15	114
		4	7/22	40
		5	8/31	130
C (sunflower)	2017	1	6/19	80
		2	6/30	80
	2018	1	6/20	140
		2	7/14	100
D (maize)	2017	1	6/13	150
		2	6/26	94
		3	7/6	50
		4	7/14	174
		5	8/6	120

444


445 Daily meteorological data, including air temperature, precipitation, relative
 446 humidity, wind speed, and sunshine duration, originated from the weather station at
 447 the Shahaoqu experimental station. The soil moisture content for the four

Was the salinity of the irrigation source water measured? Was the actual salinity of the irrigation water used in the mass balance (equation 18 of the model)?

557 60-80 cm depth (Table 2, Fig.5). Only after the last irrigation and during harvest of the
 558 crop did the moisture content in the top 0-40 cm for maize and 0-60 cm for sunflower
 559 decrease below the moisture content at -33kPa. During the growing season, the
 560 variation of moisture content was greater in the top 60 cm with the majority of the
 561 roots than in the lower depths where, after the first irrigation, it remained nearly
 562 constant close to saturation.



563
 564 **Fig. 5** Observed (blue dots) and simulated soil moisture content of the Shahaqu
 565 experimental fields during model calibration (a,b,c) and validation (d,e,f)

 Number: 1 Author: Subject: Highlight Date: 2020-06-18 20:55:56


As noted in the previous revision, it is difficult to distinguish between the blue dot markers that are in the legend from those that represent data. In five of these panels above (Figure 5), the legend lies within the data range. Possibly it would be better to use only one legend for all six panels and have it located outside the domain of the data. The same problem is observable in figure 6.

812 numerically with an implicit backward scheme and is combined by Xu et al. (2015)
813 with the EPIC model. The accuracy of our simulation results, despite the difference in
814 complexity, are very similar. The moisture contents were simulated slightly better with
815 EPICS, the groundwater depth was nearly the same, and the LAI values were
816 predicted more accurately in the SWAP-EPIC model. Xue et al. (2015) did not
817 simulate the salt content of the soil. Compared to less data and computational
818 intensive models that are applied in the Yellow River, the soil moisture content were
819 simulated more accurately by EPICS than in the North China Plain with 30 m deep
820 groundwater by surrogate models of Kendy et al. (2003) and Yang et al. (2015 a,b)
821 and in the Hetao irrigation district by Gao et al. (2017b) and Xue et al. (2018) during
822 the crop growth period.

823 **To obtain more accurate results in the future,** the upward capillary flux from
824 groundwater needs to be improved. In addition, the evapotranspiration measured
825 independently, using Eddy covariance (Zhang et al., 2012; Armstrong et al., 2008)
826 and Bowen ratio-energy balance method (Zhang et al., 2007) should be further used
827 to test performance of the model in the future study.

828 The limitation of the EPICS model is it can only be applied in areas where
829 groundwater is generally less than 3.3 m deep. When the groundwater is deeper than
830 3.3 m, the field capacity of the surface soil is determined by the moisture content
831 when the hydraulic conductivity becomes limiting and not by the depth of the
832 groundwater.

833 Overall, the present model has the advantage that it greatly simplifies the

 Number: 1 Author: Subject: Highlight Date: 2020-06-18 22:02:13

Although dilution of salinity during irrigation events seems evident in the observed data, I would still recommend adding that future refinement of the model would be served by measuring the salinity of irrigation source water. This would be more important if this model was implemented for irrigation that depends on groundwater sources, especially hydrologically closed basins.